Inkjet printing of flexible MOS structures based on graphene and high-k dielectrics

Omar Olmedo Ferrer*
MIND-IN2UB, Electronics department
Universitat de Barcelona
Martí i Franquès 1, 08028 Barcelona, Spain.

Advisors: Olga Casals, Albert Cirera

Abstract: MOS structures have been inkjet printed using silver, hafnium oxide (HfO_2) and reduced graphene oxide (rGO). Main drawbacks with inkjet printing and electrospray deposition have been overcome. C-V characteristics of these devices have been measured and common phenomenology has been established. Deviations from known theory as well as technical improvement have been proposed.

I. Introduction

MOS devices are the basic construction unit in modern electronics. They form capacitors and transistors that are the heart of processing units, where they are manufactured with monolithic technology. The main drawbacks of this process are expensive and complex equipment and the need of specific masks.

In order to overcome these difficulties, inkjet technology provides an alternative to this expensive manufacture process in which materials are only deposited where it is desired [1]. Suitable inks could be developed to print the most interesting and rare materials. Beside, ink formulations that guarantee good print quality on a wide range of substrates have been improving recently. The material to be printed can be found in different ways in the ink. Metals are usually in polymer functionalized nanoparticles (NPs) dispersed into an oil, an alcohol or water. Oxides are similar or in metal NPs that are oxidized during thermal curing process. Once one has an ink with proper characteristics for printing, essentially density, viscosity and surface tension [2], printing process is a matter of following a few established steps: preparation, calibration, alignment and printing. As a counterpart, printed electronics gives less maximum working frequency, reliability and integration density.

Flexible electronics is a technology that provides integrated circuits on a flexible substrate, usually a polyimide [3]. This technology is useful in devices that have moving parts or little room for circuitry. Another use of flexible electronics could be throwaway devices, like ID cards [4]. For example, flexible gas sensors are used inside firemen jackets and flexible antitheft alarms are used in some articles in shops, such as books, shoes and clothes [5,6].

Graphene, among other 2D materials, is probably the trendiest compound because of its good theoretical properties: high carrier mobility and heat conduction, high resistance to mechanical stress and nearly transparent [7,8]. Moreover flexibility of graphene suggests its use in flexible electronics [9].

However, expensive and complicated processes are needed to produce it, such as chemical vapor deposition (CVD), or hardly reliable and reproducible, as mechanical exfoliation of graphite [10]. Alternatively, some authors have proposed reduced graphene oxide (rGO). In recent works, rGO has been printed by inkjet technology to develop graphene based transistors [11]. Due to the difficulty of developing a rGO printable ink, we have chosen to use electrospray, a technique that allows to deposit a variety of materials [12].

In this work we present graphene-based metal-oxide-semiconductor (MOS) capacitors in a structure that combines printed silver and high-k HfO_2, and electrospray deposited rGO on Kapton®, a polyimide that is stable up to 400ºC.

As far as we know, there is no previous work dealing with printed HfO_2 and electrospray deposited rGO capacitors on Kapton® as substrate.

II. Experimental

MOS capacitors have been manufactured by inkjet printing and electrospray. First, bottom gate contacts have been printed on sheets of Kapton® 50μm thick using SunChemical® silver ink in Xennia® Xenjet™ 4000 inkjet printer. Two types of capacitors have been printed, as seen in figure 1(a) and 1(b). Then, Torrecid® HfO_2 ink has been printed on top of the silver contacts, covering completely the silver in type

* oolmedo@el.ub.edu

1 capacitors and in a square as wide as the contact in type 2. Different thicknesses of HfO_2 have been deposited by printing up to 4 layers, as seen in table 1. Each inkjet printing is sintered via thermal curing in a muffle, where temperature and curing time depends on ink specifications. Essentially, the curing process consists of 220ºC during 20 minutes for silver and 240ºC during 20 minutes for hafnium oxide.

Yflow® Electrospinner 3.2.D-400® has been used to deposit rGO by electrospray on top of the oxide. The dispersion used consists on 10mg of Graphenea® rGO powder in 40ml of isopropanol. rGO is produced by Hummers method, which consist on chemical and thermal attack of graphite powder, and a subsequent chemical reduction [13,14]. Deposition conditions can be found in table 1.

In type 1 capacitors, smaller silver squares have been printed on top of rGO deposit to make an electric contact.

Sample	HfO_2 layers	rGO deposit time (min)	Type
3591	3	25	1
3592	3	30	1
3593	3	35	1
3594	3	40	1
3907-A3	2	20	1
3907-A4	2	20	1
3909-B2	3	20	1
3909-C2	3	20	1
3915-T	4	35	2
3916-B	2	35	2
3917-T	1	25	2
3917-B	1	35	2
3918-T	2	25	2
3918-B	2	35	2
3937-T	4	20	2
3937-B	3	25	2
3938-T	1	20	2
3938-B	1	20	2
3939-T	2	25	2
3939-B	2	25	2
3940-T	4	25	2
3940-B	3	35	2
3941-T	1	25	2
3941-B	1	35	2
3974-B	SiO_2	35	R
3974-S	SiO_2	35	R
3975-B	SiO_2	25	R
3975-S	SiO_2	25	R

Table 1: sample experimental parameters. On samples 3915 to 3940, T stands for Top and B stands for Bottom, since there are two capacitors in each sample. Similarly, on samples 3974 and 3975, B stands for Big and S stands for Small.

Reference MOS capacitors (3974-B, 3974-S, 3975-B and 3975-S) were also printed using ANP® silver ink for the bottom gate and Politronica® SiO_2 ink for the dielectric, in order to compare oxide behaviours. These capacitors can be seen in figure 1(c).

Inkjet printing process showed many difficulties due to incompatibility among inks. An example is clearly shown in figure 1(a) where wettability of top silver contact exceeded by far desired pattern.

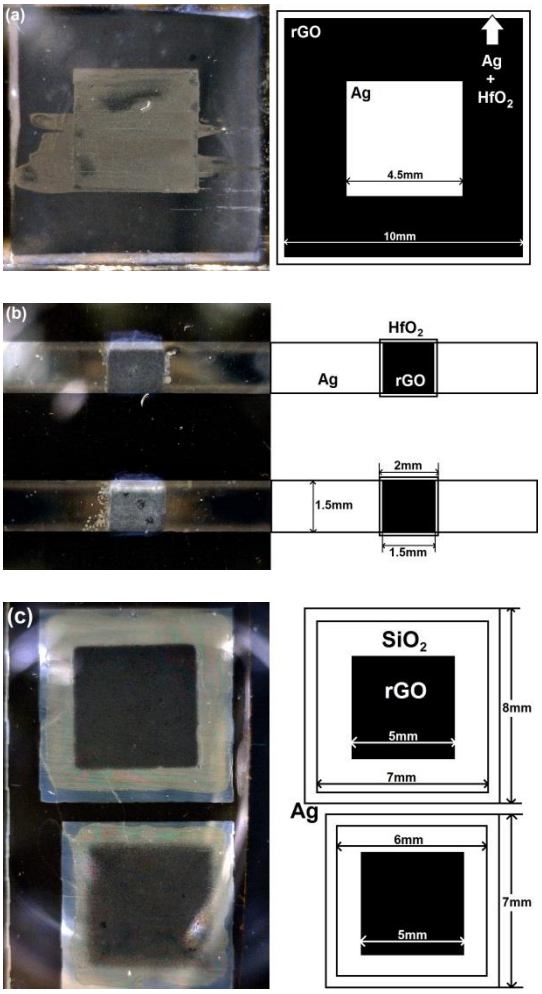

Figure 1: three types of capacitors manufactured. (a) Sample 3593, type 1 $Ag/HfO_2/rGO/Ag$ capacitor, (b) sample 3940, type 2 $Ag/HfO_2/rGO$ capacitors and (c) sample 3974, $Ag/SiO_2/rGO$ reference capacitors.

Samples were observed by scanning electron microscope (SEM) using a Jeol JSM-6510. For the electrical characterization, C-V characteristics of the MOS capacitors have been obtained by Keithley® 4200-SCS impedance analyser. The system measures the modulus and phase of the impedance and then computes the equivalent capacitance and conductance using a model that consists on a capacitor and a resistor in parallel (C_P-G_P model). Some C-V plots showed negative capacities, which is the equivalent to having inductive effects in this model.

III. Results and discussion

Samples of Ag/HfO_2/rGO MOS capacitors have been observed by SEM in order to examine the uniformity of the films and to confirm the deposition of rGO.

Bottom contacts have been examined to determine the state of the silver. Figure 2(a) shows that silver ink is well sintered and smooth. Some graphene flakes clusters can be seen too, darker in backscattered electrons (BSE) image on the inset.

An image of the oxide deposit is shown in figure 2(b). It shows cracks between micrometric grains, what may lead to a leakage current through the oxide. They could be due to a partial crystallization during thermal curing of the ink or by the mechanical stress to which the sample is subjected during the different stages of manufacture. However, integrity of HfO_2 has been checked previously in MIND group by cross section SEM assisted by FIB after printing it on a silicon wafer, not showing cracks.

Silver top contact of sample 3591 shows two distinct types of deposit, one metallic and another matte white. Images of this contact have been taken in order to establish microscopic differences between these two zones. It can be seen on images 2(c) and 2(d). While metallic silver is smooth and covers most of the oxide, matte white one looks cracked and patchy. These differences may be caused by the remaining isopropanol from electrospray process. This residue may alter the stability of top printed silver ink and worsen its appearance and conductive properties. Later in the electrical characterization it was found that top printed silver diffuses through the oxide. For this reason, connection with the impedance analyzer's gold tips was made directly on rGO.

rGO deposit has been observed in order to determine its uniformity. It can be seen in figure 3 that rGO flakes deposited by electrospray are in micrometric accumulations and they are more of these clusters when electrospray time is longer, as one can extract from the comparison between figures 3(a) and 3(b), where the first one corresponds to an electrospray time of 25 minutes and the second one to 40 minutes. The different quantity of these accumulations is more evident in BSE images, shown in the insets of figures 3(a) and 3(b). Flakes are not totally connected and hafnium oxide, cracked in some regions, can be seen through the deposit.

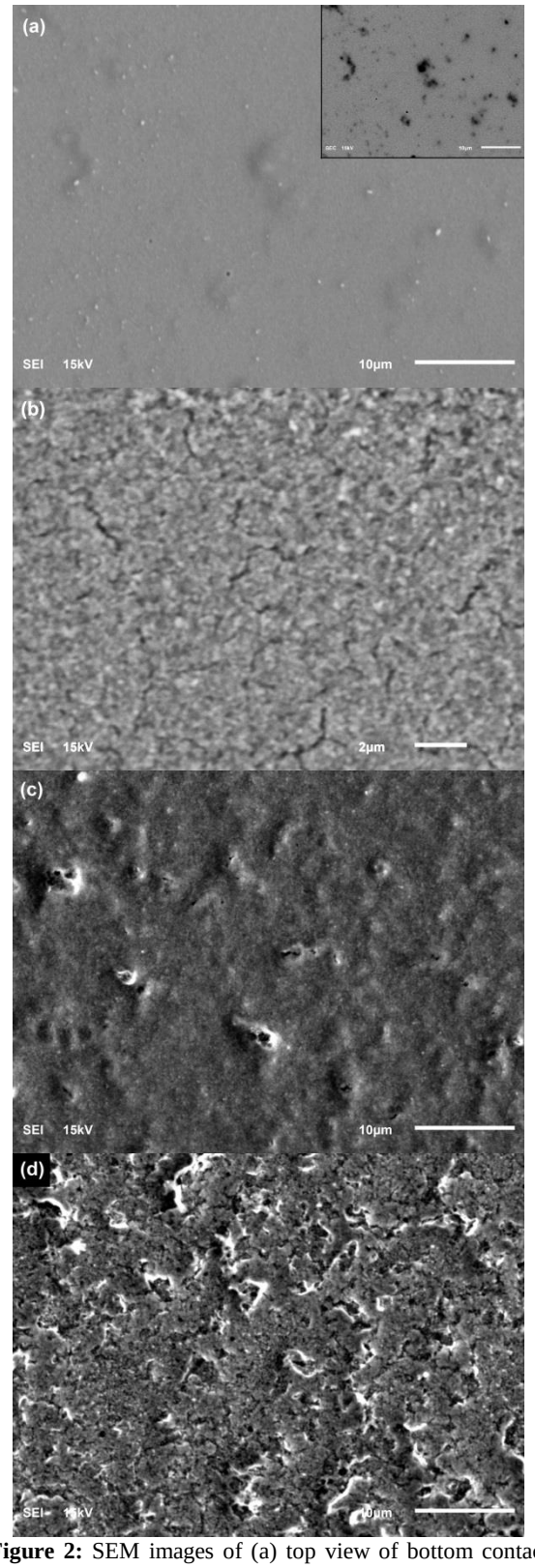

Figure 2: SEM images of (a) top view of bottom contact silver of sample 3915-T, BSE image inset showing rGO accumulations in black, (b) HfO_2 deposit with cracks, sample 3915-T, (c) top contact metallic silver, sample 3591, and (d) top contact matte white silver, patchy and cracked, sample 3591.

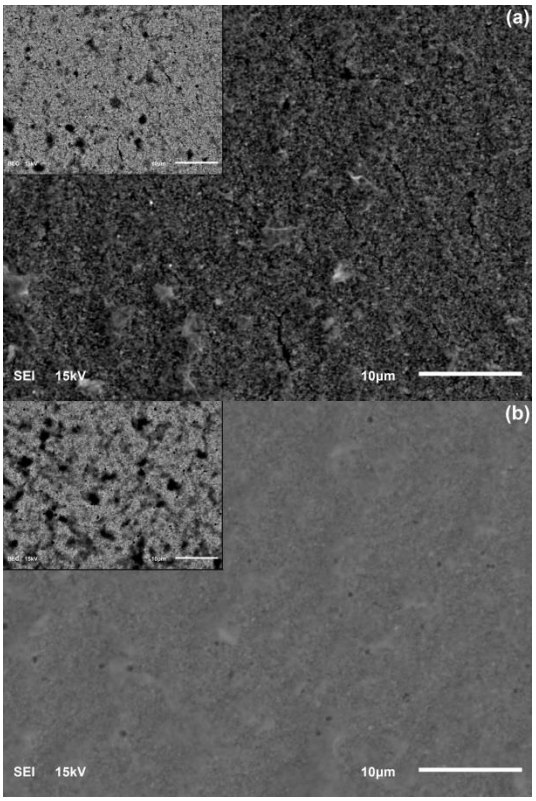

Figure 3: SEM images of (a) rGO deposit on sample 3591, 25 minutes of rGO electrospray and (b) rGO deposit on sample 3594, 40 minutes of rGO electrospray. Insets show the same region in BSE imaging mode of SEM.

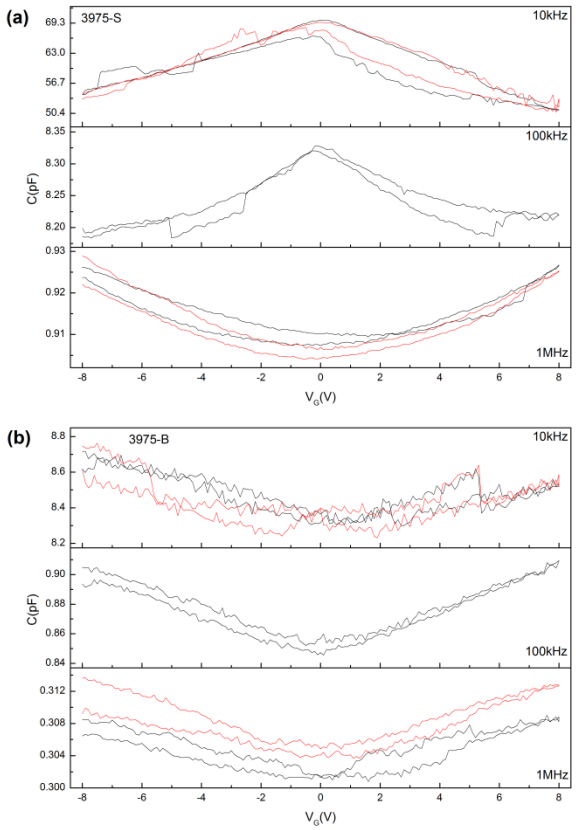

Figure 4: C-V curves of Ag/SiO_2/rGO MOS devices. (a) Sample 3975-S, Fuji mount shaped C-V at low frequencies and (b) sample 3975-B, low rGO thickness behaviour.

Concerning the electrical characterization, let us start showing reference capacitors by SiO_2. Two different behaviors have been observed in Ag/SiO_2/rGO MOS structures. Some of them show Fuji mount shaped C-V curves at low frequencies, as seen in figure 4(a). When rGO thickness is extremely low, as it can be found in figure 4(b), capacity increases with gate bias. One can attribute this behavior to rGO, since it is also found in HfO_2 MOS capacitors shown below.

Concerning HfO_2 MOS capacitors, type 1 devices were unable to be tested by contacting top silver contacts because diffusion of silver though graphene and oxide. Therefore, devices were tested connecting with the impedance analyzer's gold tips on rGO.

Some of the Ag/HfO_2/rGO devices show a sort of MOS-like C-V curve at high frequencies, as shown in figure 5. These curves show hysteresis when the voltage sweep is done forward and reverse. This is the typical effect shown in a MOS capacitor with mobile charges inside the oxide, which is the case of HfO_2 [15].

It is interesting to notice that devices in figure 5 are samples with thick layers of rGO and hafnium oxide. Samples with thinner layers of HfO_2 and rGO show similar hysteresis but with less intensity, as can be seen in figure 6. Finally, samples in figure 7, the ones with the smallest amount of oxide and rGO do not show hysteresis considering the technical limitations of measurement.

These results suggest a relation between thickness and hysteresis. The trend suggests higher accumulation of charges with printed and electrospray deposited layers. A simple explanation would suggest rests of deposition, mainly solvents, as mobile charges responsible of hysteresis.

Because of the limited number of samples, it is not possible to do statistics and clarify if the above described effect is due to oxide or rGO. The main difficulty in making many identical devices is electrospray. With this technique, rGO layer may undergo deposition conditions changes during deposition. Besides, alignment and calibration errors during inkjet printing difficult the whole reproducibility of samples.

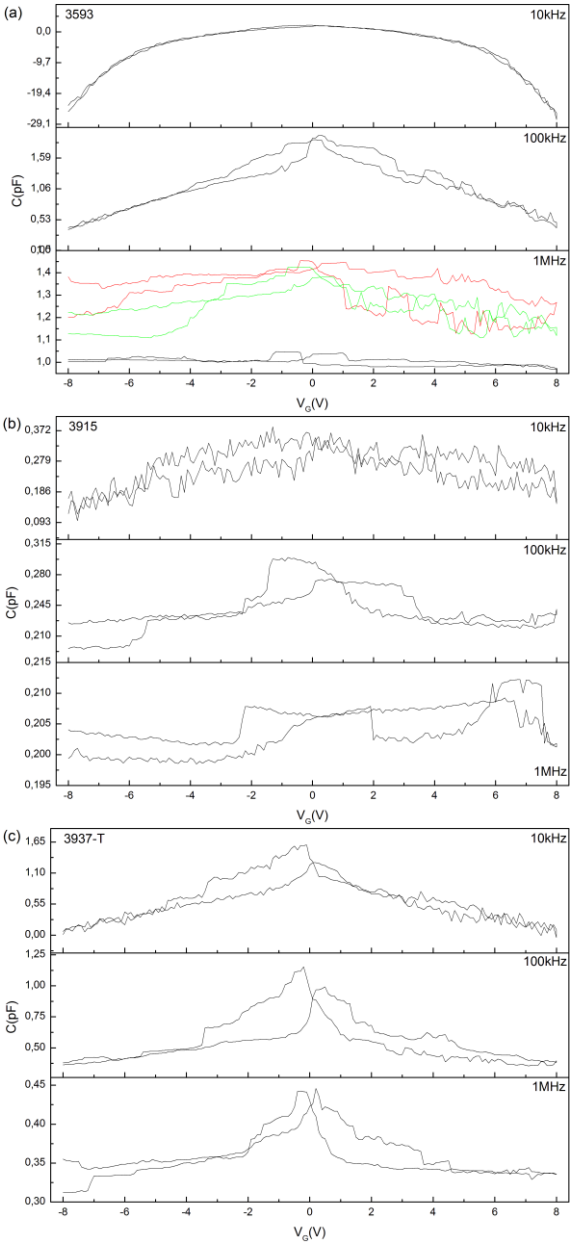

Figure 5: Samples showing MOS-like hysteresis in C-V curves. (a) 3593, type 1, (b) 3915, type 2 and (c) 3937-T, type 2.

The expected behavior of an ideal MOS capacitor is shown in figure 8. As can be seen, high frequency curve takes account of oxide capacity in accumulation region (-*V*) and of series combination of oxide and depleted zone of semiconductor capacities in inversion region (+*V*), as seen on the following formula:

$$C_{min} = \frac{C_i C_D}{C_i + C_D}$$

where C_i and C_D are oxide and depletion capacities, respectively [16].

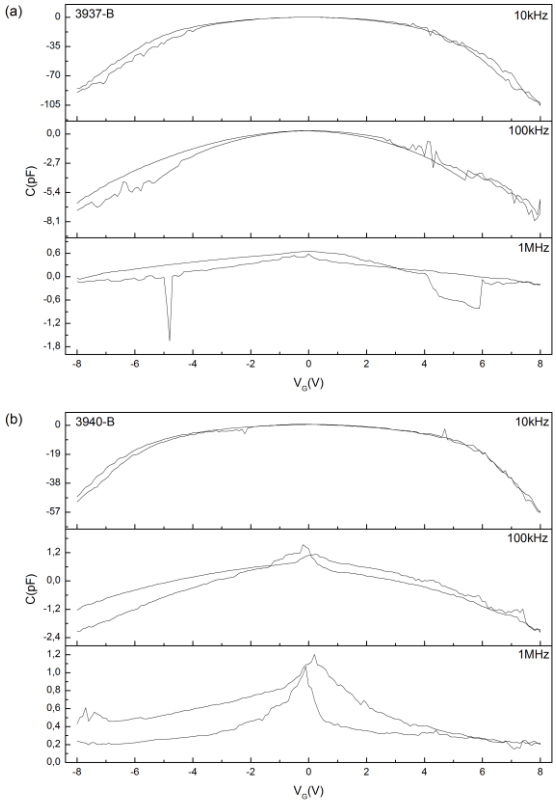

Figure 6: Samples showing less MOS-like hysteresis in C-V curves. (a) 3937-B and (b) 3940-B, both type 2.

One can observe that C-V characteristics of studied devices deviate much from the expected. This is because printed and thin film capacitors are far away of ideal models. On one hand, both printed and high-k oxides show larger amounts of trapped and mobile charges in them than monolithic oxides, and on the other hand we do not know which is the effective doping of this type of graphene. It could be P-doped if it is not totally reduced, because chemical groups with oxygen accept electrons, or it could be N-doped due to the interaction with mobile ions in the oxide interface. Even it could change its doping depending on the movement of charges inside or on the surface of the oxide. In the light of these results, more complex models have to be used to understand the devices that we deal with [17,18].

Another explanation of the unclear MOS effect could the rGO acting as a metal. If the band gap of rGO is small enough, there could be a large amount of carriers and our device should behave as a MIM capacitor. The C-V curve of a MIM capacitor is expected to be quadratic and this seems to be closer to our results when oxide and rGO films are thinner. Even so, deviations from this model are also observable and they could be again due to impurities in the layers driving to trapped or mobile charges in oxide or due to changes in the amount of carriers in rGO layer.

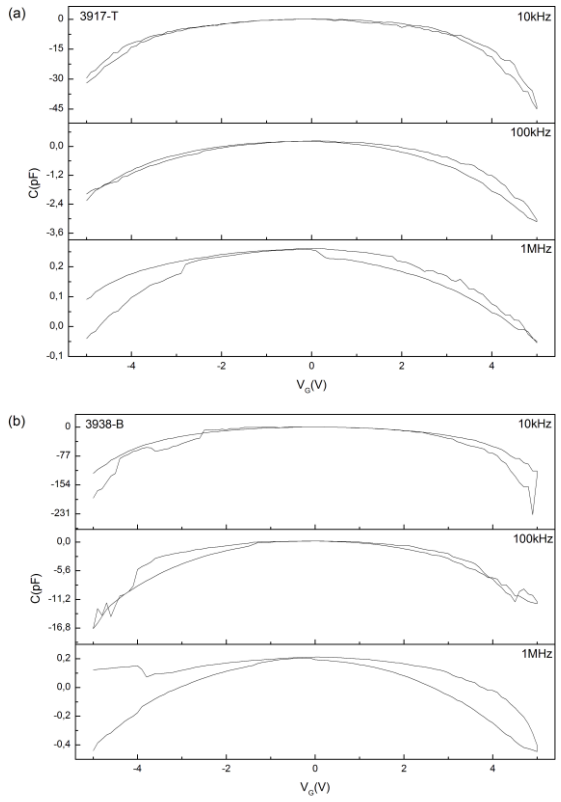

Figure 7: Samples not showing MOS-like behaviour. (a) 3917-T and (b) 3938-B, both type 2.

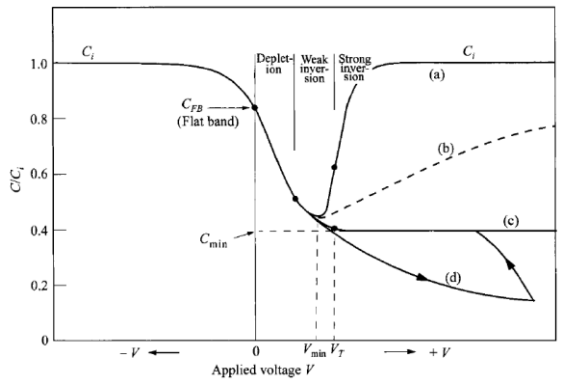

Figure 8: N-MOS capacitor C-V curves: (a) low frequency, (b) medium frequency, (c) high frequency and (d) high frequency with fast sweep (deep depletion).

IV. Conclusions

The following conclusions have been drawn after this work:

- Flexible MOS structures have been manufactured combining inkjet printing and electrospray, resulting in Ag/HfO_2/rGO devices.
- Main problems of this type of device construction have been found and these are alignment of inkjet processes and irreproducibility and slowness of electrospray deposition.
- C-V characteristics of the devices have been measured and common behaviors have been observed.
- Deviation from ideal models has been observed. Reasons for this deviation have been proposed.

Taking into account the research previously exposed in this work, the author suggests the following steps:

- Systematic device manufacturing varying thickness of different layers and in sufficient quantity to do statistics.
- Electrospray rGO tracks on top of different substrates to deduce its conductivity and uniformity.
- Section imaging of the structures with SEM and TEM to know thicknesses of silver, oxide and rGO films.
- EDX mapping in SEM, EELS in TEM or XPS have to be done to analyze if there is diffusion of layers into the others [19].
- Inkjet printing of rGO to achieve full-inkjet devices and make manufacturing more simple and reproducible.

V. Acknowledgments

I want to thank my advisor Albert Cirera for the advice and support given during this work and Olga Casals for the aid on theoretical background.

Thanks to Giovanni Vescio for the training with the inkjet equipment, encouragement and dedication.

Thanks to Aida Varea for training with electrospray and assistance in SEM, as well as general advice while writing this report.

Finally, thanks to Xavi Arrese, Oriol Monereo, Bea Medina and the rest of lab mates for the companionship and friendship they offered to me during last months.

VI. References

[1] M. Singh, H. M. Haverinen, P. Dhagat, and G. E. Jabbour, Adv. Mater. **22**, 673 (2010).

[2] E. Tekin, P. J. Smith, and U. S. Schubert, Soft Matter **4**, 703 (2008).

[3] H. Yan, Z. Chen, Y. Zheng, C. Newman, J. R. Quinn, F. Dötz, M. Kastler, and A. Facchetti, Nature **457**, 679 (2009).

[4] Y.-Y. Noh, N. Zhao, M. Caironi, and H. Sirringhaus, Nat. Nanotechnol. **2**, 784 (2007).

[5] O. Monereo, S. Claramunt, M. M. De Marigorta, M. Boix, R. Leghrib, J. D. Prades, a Cornet, P. Merino, C. Merino, and a Cirera, Talanta **107**, 239 (2013).

[6] S. Claramunt, O. Monereo, M. Boix, R. Leghrib, J. D. Prades, a. Cornet, P. Merino, C. Merino, and a. Cirera, Sensors Actuators B Chem. **187**, 401 (2013).

[7] P. Avouris, Nano Lett. 4285 (2010).

[8] M. J. Allen, V. C. Tung, and R. B. Kaner, Chem. Rev. **110**, 132 (2010).

[9] A. Varea, E. Xuriguera, B. Medina, S. Claramunt, O. Monereo, and A. Cirera, in *Eur. Mater. Res. Soc.* (2014).

[10] K. Lakshmi Ganapathi, N. Bhat, and S. Mohan, Appl. Phys. Lett. **103**, 073105 (2013).

[11] F. Torrisi, T. Hasan, W. Wu, Z. Sun, A. Lombardo, T. S. Kulmala, G. W. Hsieh, S. Jung, F. Bonaccorso, P. J. Paul, D. Chu, and A. C. Ferrari, ACS Nano **6**, 2992 (2012).

[12] a. Jaworek, J. Mater. Sci. **42**, 266 (2006).

[13] S. Pei and H.-M. Cheng, Carbon N. Y. **50**, 3210 (2012).

[14] S. Mao, H. Pu, and J. Chen, RSC Adv. **2**, 2643 (2012).

[15] H.-Y. Guo and Z.-G. Ye, Mater. Sci. Eng. B **120**, 68 (2005).

[16] S. M. Sze and K. K. Ng, *Physics of Semiconductor Devices*, 3rd edition (2006).

[17] H. Xu, Z. Zhang, and L.-M. Peng, Appl. Phys. Lett. **98**, 133122 (2011).

[18] K. Martens, C. O. Chui, G. Brammertz, B. De Jaeger, D. Kuzum, M. Meuris, M. Heyns, T. Krishnamohan, K. Saraswat, H. E. Maes, and G. Groeseneken, IEEE Trans. Electron Devices **55**, 547 (2008).

[19] T.-T. Tan, Z.-T. Liu, and Y.-Y. Li, Chinese Phys. Lett. **28**, 086803 (2011).